Langmuir
Article
pubs.acs.org/Langmuir

Microfluidic Fabrication of Porous Polymer Microspheres: Dual Reactions in Single Droplets

Xiuqing Gong, Weijia Wen,* and Ping Sheng

Department of Physics and KAUST-HKUST Micro/Nano-fluidics Joint Laboratory, The Hong Kong University of Science and Technology, Clear Water Bay, Kowloon, Hong Kong

Received January 13, 2009. Revised Manuscript Received April 8, 2009

We report the microfluidic fabrication of macroporous polymer microspheres via the simultaneous reactions within single droplets, induced by UV irradiation. The aqueous phase of the reaction is the decomposition of H_2O_2 to yield oxygen, whereas the organic phase is the polymerization of NOA 61, ethylene glycol dimethacrylate (EGDMA), and tri (propylene glycol) diacrylate (TPGDA) precursors. We first used a liquid polymer precursor to encapsulate a multiple number of magnetic Fe_3O_4 colloidal suspension (MCS) droplets in a core−shell structure, for the purpose of studying the number of such encapsulated droplets that can be reliably controlled through the variation of flow rates. It was found that the formation of one shell with one, two, three, or more encapsulated droplets is possible. Subsequently, the H_2O_2 solution was encapsulated in the same way, after which we investigated its decomposition under UV irradiation, which simultaneously induces the polymerization of the encapsulating shell. Because the H_2O_2 decomposition leads to the release of oxygen, porous microspheres were obtained from a combined H_2O_2 decomposition/polymer precursor polymerization reaction. The multiplicity of the initially encapsulated H_2O_2 droplets ensures the homogeneous distribution of the pores. The pores inside the micrometer-sized spheres range from several micrometers to tens of micrometers, and the maximum internal void volume fraction can attain 70%, similar to that of high polymerized high internal phase emulsion (polyHIPE).

Introduction

There are various forms of porous polymers which can include microporous polymers, mesoporous polymers, macroporous polymers, and, according to their pore size, polymerized high internal phase emulsions (polyHIPE). The microporous, mesoporous, and macroporous polymers have pore diameters of less than 2 nm, between 2 and 50 nm, and greater than 50 nm, respectively, as defined by IUPAC.[1−4] The pore formation is usually a process of phase separation either in suspension polymerization or swelling and polymerization. The control variables of pore size mainly include the effect of the cross-linking monomer and porogen, the reaction temperature, swelling ratio of seed polymer, etc.[5−10] PolyHIPE are characterized by the presence of larger cavities (as opposed to pores), the sizes of which can vary over a 1 μm- to millimeter-scale range, but the majority of polyHIPE have cavities that are tens of micrometers in diameter. These cavities are interconnected by a series of smaller pores that enable them to communicate with adjacent cavities. HIPEs are emulsions in which the interior phase occupies at least 74% of the volume of the emulsion. Water, an initiator, and a suitable salt are first mixed together to constitute the interior phase. This interior phase is mixed with the organic phase and emulsified (with a suitable emulsifier) to form a water-in-oil (WO) HIPE in which the emulsified water droplets are uniformly dispersed inside the continuous phase composed of monomer, solvent, and surfactant. Polymerization of the continuous phase and the removal of the aqueous droplets (by drying) lead to the formation of highly porous structure.[11−15] Fabricating polyHIPE with symmetric spherical geometry and controlled porosity is of particular interest because they allow for diversified applications in chromatography, adhesives, cell culture, drug delivery, catalysis, and enzyme immobilization, among others.[16−21]

Recent developments in microfluidics have met partial success in continuous preparation of monodisperse polymer microspheres with a controlled narrow distribution by UV-induced polymerization, e.g., the preparation of polyEGDMA, polyTPGDA, or their copolymer.[22−24] The first step to prepare such microspheres is commonly known as the emulsification process, which entails the

*Corresponding author. E-mail: phwen@ust.hk.

(1) Hentze, H. P.; Antonietti, M. *Rev. Mol. Biotechnol.* **2002**, *90*, 27–53.
(2) Xie, S. F.; Allington, R. W.; Fréchet, J. M.; Svec, F. *Adv. Biochem. Eng. Biotechnol.* **2002**, *76*, 87–125.
(3) Lumelsky, Y. L.; Zoldan, J.; Levenberg, S.; Silverstein, M. S. *Macromolecules* **2008**, *41*, 1469–1474.
(4) Macintyre, F. S.; Sherrington, D. C. *Macromolecules* **2004**, *37*, 7628–7636.
(5) Svec, F.; Fréchet, J. M. J. *Science* **1996**, *273*, 205–211.
(6) Sherrington, D. C. *Chem. Commun.* **1998**, 2275–2286.
(7) Jose, A. J.; Ogawa, S.; Bradley, M. *Polymer* **2005**, *46*, 2880–2888.
(8) Durie, S.; Jerabek, K.; Mason, C.; Sherrington, D. C. *Macromolecules* **2002**, *35*, 9665–9672.
(9) Shastri, V. P.; Martin, I.; Langer, R. *Proc. Natl. Acad. Sci. U.S.A.* **2000**, *97*, 1970–1975.
(10) Ogino, K.; Sato, H.; Tsuchiya, K.; Suzuki, H.; Moriguchi, S. *J. Chromatogr.* **1995**, *699*, 59–66.
(11) Cameron, N. R. *Polymer* **2005**, *46*, 1439–1449.
(12) Kulygin, O.; Silverstein, M. S. *Soft Matter* **2007**, *3*, 1525–1529.
(13) Zhang, H. F.; Cooper, A. I. *Soft Matter* **2005**, *1*, 107–113.
(14) Zhang, H. F.; Long, J.; Cooper, A. I. *J. Am. Chem. Soc.* **2005**, *127*, 13482–13483.
(15) Butler, R.; Davies, C. M.; Cooper, A. I. *Adv. Mater.* **2001**, *13*, 1459–1463.
(16) Righetti, P. G. *J. Chromatogr. A* **1995**, *698*, 3–17.
(17) Sellergren, B. *Angew. Chem., Int. Ed.* 2000, *39*, 1031−1037.
(18) Busby, W.; Cameron, N. R.; Jahoda, C. A. *Biomacromolecules* **2001**, *2*, 154–164.
(19) Ashton, R. S.; Banerjee, A.; Punyani, S.; Schaffer, D. V.; Kane, R. S. *Biomaterials* **2007**, *28*, 5518–5525.
(20) Zhang, H. F.; Cooper, A. I. *Adv. Mater.* **2007**, *19*, 2439–2444.
(21) Haratake, M.; Yasumoto, K.; Ono, M.; Akashi, M.; Nakayama, M. *Anal. Chim. Acta* **2006**, *561*, 183–190.
(22) Seo, M.; Nie, Z.; Xu, S.; Mok, M.; Lewis, P. C.; Graham, R.; Kumacheva, E. *Langmuir* **2005**, *21*, 11614–11622.
(23) Xu, S.; Nie, Z.; Seo, M.; Lewis, P.; Kumacheva.; Stone, H. A.; Garstecki, P.; Weibel, D. B.; Gitlin, I.; Whitesides, G. M. *Angew. Chem., Int. Ed.* **2005**, *44*, 724–728.
(24) Dubinsky, S.; Zhang, H.; Nie, Z.; Gourevich, I.; Voicu, D.; Deetz, M.; Kumacheva, E. *Macromolecules* **2008**, *41*, 3555–3561.

serial formation of single symmetric droplets in a continuous immiscible phase, using either the "T" junction geometry or a microfluidic flow-focusing (MFF) device.[25−28] This step allows an emulsion, for example, W/O (water droplets in oil) or O/W (oil droplets in water).[29] Then an UV irradiation is applied to solidify the droplets in emulsion. If another emulsification process is added which uses another immiscible fluid (carrying fluid) to further shear the W/O or O/W emulsion, core−shell droplets of either W/O/W or O/W/O structure can be formed.[30−34] The carrying fluid carries droplets of emulsion through the channel, resulting in the formation of multiple emulsions (emulsions of emulsions[8]) and subsequent core−shell microspheres after solidification.[35]

Recently, Li et al. reported a synergism of two reactions in a single droplet by microfluidics, the first reaction being the exothermic free radical polymerization of an acrylate monomer and the second one the endothermic polycondensation of a urethane oligomer. The heat generated from the first reaction triggers the subsequent polymerization, leading to the formation of an interpenetrating polymer network (IPN). The pore size is on the order of hundreds of angstroms and resembles the structure of a macroporous polymer.[36] Dubinsky et al. also reported the fabrication of macroporous polymer by introducing porogen solvents into microfluidics. The pore sizes in that case ranged from hundreds to thousands of angstroms.[37] In the present study, we introduced the HIPE concept into microfluidics by first forming HIPE in an MFF device and then shear the HIPE into droplets. The HIPE was composed of micrometer-sized H_2O_2 droplets in polymer precursors, and the HIPE droplets are formed by shearing HIPE with other immiscible fluids (carrying fluids). To accomplish the emulsion process, we modified the MFF device by decreasing the channel size while increasing the channel length of the emulsion area in order to allow more time for emulsification. This design leaves us enough space to better control the factors within the emulsification process, such as the droplet number and size. In order to determine the design's feasibility, we initially used photocurable NOA 61 precursor to encapsulate droplets of magnetic Fe_3O_4 colloidal suspension (MCS) and study the manner in which one can control the formation of encapsulated droplets' number by varying the flow rate. We found that after solidification the polymeric shell can contain one, two, or multiple magnetic cores. Accordingly, we replaced the MCS with hydrogen peroxide (H_2O_2) solution, forming the internal phase inside the NOA 61 precursor. The H_2O_2 can be decomposed

Scheme 1. Polymerization of (a) NOA 61,[44,45] (b) EGDMA, and (c) TPGDA Precursor under the Application of UV Irradiation

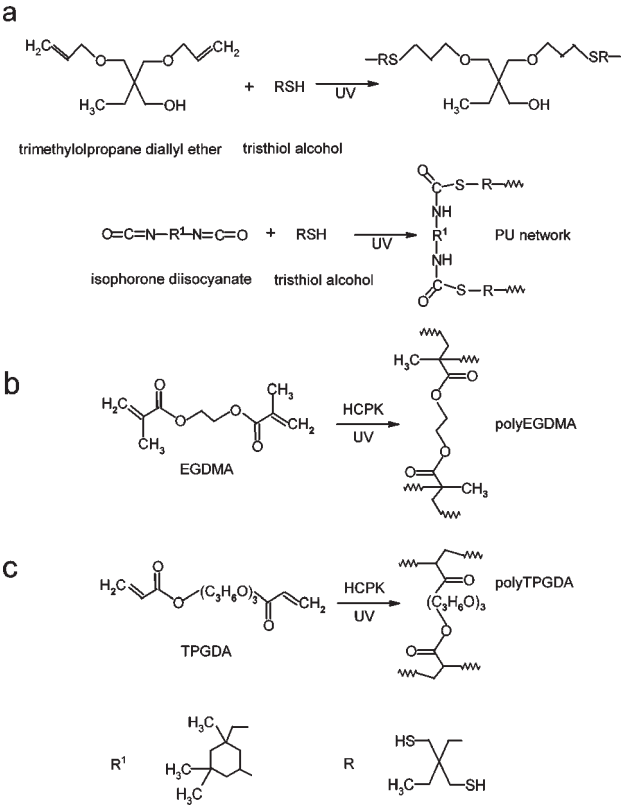

under UV irradiation.[38−41] During the course of the UV irradiation, the polymer precursor was also gradually solidified through the photopolymerization reaction (Scheme 1a). As the decomposition of H_2O_2 creates oxygen that has to be released through the polymerized shell, pores are formed, extending to the surface. By this method, we also fabricated porous microspheres of acrylate-based monomers, ethylene glycol dimethacrylate (EGDMA), and tripropylene glycol diacrylate (TPGDA, Scheme 1b,c).

Experimental Section

Materials. Silicon elastomer base and curing agent used to prepare the MFF chip were obtained from Dow Corning Corp. The photocurable NOA 61 precursor was available as optical adhesive from Norland Inc. The NOA series adhesive comprising thiolene monomer liquid is a mixture of trimethylolpropane diallyl ether, trimethylolpropane tristhiol, isophorone diisocyanate ester, and a benzophenone photoinitiator.[42−45] Paraffin (kinematic viscosity ≥ 34.5 cSt at 40 °C) and high molecular weight chitosan, with a viscosity of 800 cP and degree of deacetylation of 75%, were obtained from Sigma. FITC (95+ % isomer) was purchased from International Laboratory. EGDMA (M_w 198.22, Sigma) and TPGDA (mixture of isomers, M_w 300.35, Sigma) precursors were prepared by respectively mixing EGDMA and TPGDA with 4 wt % of photoinitiator 1-hydroxycyclohexyl phenyl ketone (HCPK, Aldrich), 1 wt % of poly(ethylene glycol) methyl ether methacrylate (PEGMEM, average M_n 1100, Aldrich), and 2 wt % of sorbitan monooleate

(25) Nisisako, T.; Torii, T.; Higuchi, T. *Lab Chip* **2002**, *2*, 24–26.
(26) Garstecki, P.; Fuerstman, M. J.; Stone, H. A.; Whitesides, G. M. *Lab Chip* **2006**, *6*, 437–446.
(27) Takeuchi, S.; Garstecki, P.; Weibel, D. B.; Whitesides, G. M. *Adv. Mater.* **2005**, *17*, 1067–1072.
(28) Garstecki, P.; Stone, H. A.; whitesides, G. M. *Phys. Rev. Lett.* **2005**, *94*, 164501.
(29) Kim, J. W.; Utada, A. S.; Fernández-Nieves, A.; Hu, Z.; Weitz, D. A. *Angew. Chem., Int. Ed.* **2007**, *46*, 1819–1822.
(30) Utada, A. S.; Lorenceau, E.; Link, D. R.; Kaplan, P. D. Stone, H. A. Weitz, D. A. *Science* **2005**, *308*, 537−541.
(31) Chu, L.; Utada, A. S.; Shah, R. K.; Kim, J. W.; Weitz, D. A. *Angew. Chem., Int. Ed.* **2007**, *46*, 8970–8974.
(32) Nisisako, T.; Okushima, S.; Torii, T. *Soft Matter* **2005**, *1*, 23–27.
(33) Anna, S. L.; Bontoux, N.; Stone, H. A. *Appl. Phys. Lett.* **2003**, *82*, 364–366.
(34) Seo, M.; Paquet, C.; Nie, Z.; Xu, S.; Kumacheva, E. *Soft Matter* **2007**, *3*, 986–992.
(35) Nie, Z.; Xu, S.; Seo, M.; Lewis, P. C.; Kumacheva, E. *J. Am. Chem. Soc.* **2005**, *127*, 8058–8063.
(36) Li, W.; Pham, H. H.; Nie, Z.; MacDonald, B.; Güenther, A.; Kumacheva, E. *J. Am. Chem. Soc.* **2008**, *130*, 9935–9941.
(37) Dubinsky, S.; Zhang, H.; Nie, Z.; Gourevich, I.; Voicu, D.; Deetz, M.; Kumacheva, E. *Macromolecules* **2008**, *41*, 3555–3561.
(38) Hunt, J. P.; Taube, H. *J. Am. Chem. Soc.* **1952**, *74*, 5999–6002.
(39) Zuo, Y.; Hoigné, J. *Science* **1993**, *260*, 71–73.
(40) Faust, B. C.; Anastasio, C.; Allen, J. M.; Arakaki, T. *Science* **1993**, *260*, 73–75.
(41) Yu, X.; Barker, J. *J. Phys. Chem. A* **2003**, *107*, 1325–1332.
(42) Bhargava, R.; Wang, S. Q.; Koenig, J. L. *Macromolecules* **1999**, *32*, 2748–2760.
(43) Natali, M.; Begolo, S.; Carofiglio, T.; Mistura, G. *Lab Chip* **2008**, *8*, 492–494.
(44) Chiou, B. S.; Khan, S. A. *Macromolecules* **1997**, *30*, 7322.
(45) Chiou, B. S.; English, R. J.; Khan, S. A. *Macromolecules* **1996**, *29*, 5368.

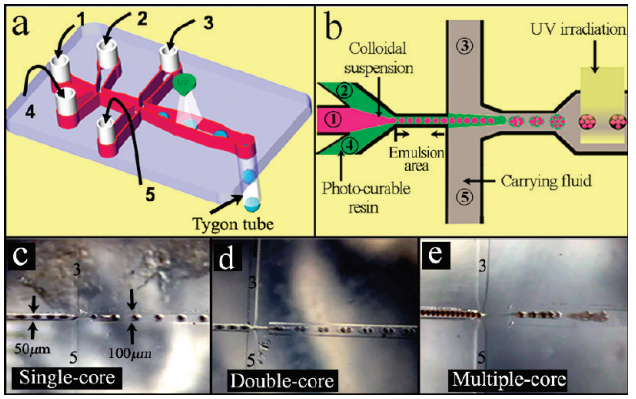

Figure 1. (a) Schematic diagram of PDMS chip fabricated by soft lithography and (b) the flowchart to illustrate the formation of NOA 61 precursor encapsulating multiple droplets. Formation of NOA 61 precursor with (c) single (Q_1 0.003 mL/h; $Q_2 = Q_4$ 0.006 mL/h; $Q_3 = Q_5$ 0.012 mL/h), (d) double (Q_1 0.003 mL/h; $Q_2 = Q_4$ 0.006 mL/h; $Q_3 = Q_5$ 0.008 mL/h), (e) multiple encapsulated magnetic aqueous droplets (Q_1 0.003 mL/h; $Q_2 = Q_4$ 0.006 mL/h; $Q_3 = Q_5$ 0.004 mL/h).

(SPAN 80, M_w 428.6, Sigma). To prepare the MCS, we first prepared Fe_3O_4 nanoparticles by a coprecipitation method detailed by Massart and as in our previous work.[46,47] Then 2.5 g of Fe_3O_4 nanoparticles was dispersed into 150 mL of acetic acid aqueous solution (2% w/v) and high-molecular-weight chitosan (1.5% w/v). Here, the addition of high-molecular-weight chitosan into MCS is to increase the viscosity of aqueous solution which helps stabilize the MCS droplets. The H_2O_2 solution was prepared by dissolving 7 g of poly(vinyl alcohol) (PVA, 95% hydrolyzed with average M_w 95 000, Acros Organics) into 100 mL of hydrogen peroxide (30 wt %, Riedel-deHaën). PVA served as emulsion stabilizer that can decrease the surface tension of the fluids and prevent the collision and breakage of H_2O_2 droplets as they were formed in the emulsion channel area and stacked in the final droplets.[48−50] The droplet size decreases with increasing PVA concentration.[49] A plateau in droplet size, 5 μm, is reached at a PVA concentration of 7 wt %. But if the concentration is above, the shearing phenomenon of H_2O_2 aqueous solution became unstable and uncontrollable foam was created.[51]

Microfluidic Fabrication. A polydimethylsiloxane (PDMS) chip with a designed pattern was fabricated by the soft-lithography method,[52,53] as schematically shown in Figure 1a. The internal phases flowing through inlet 1 comprised MCS and H_2O_2 solution. The outer phases flowing through inlets 2 and 4 included NOA 61, EGDMA, and TPGDA precursor. To prepare the NOA 61 microspheres, we used liquid paraffin as carrying fluid to flow through inlets 3 and 5, whereas to prepare the polyEGDMA and polyTPGDA microspheres, we used silicon oil (kinematic viscosity ≥ 50 cSt at 25 °C) as carrying fluid. All the chemicals were loaded into 3 mL syringe before connecting to microfluidic chip. We used three syringe pumps to control the flow rates into inlets 1 (Q_1), 2 and 4 ($Q_2 = Q_4$), and 3 and 5 ($Q_3 = Q_5$). After the microspheres were solidified and collected, they were filtered and washed with isopropanol and water. The FITC

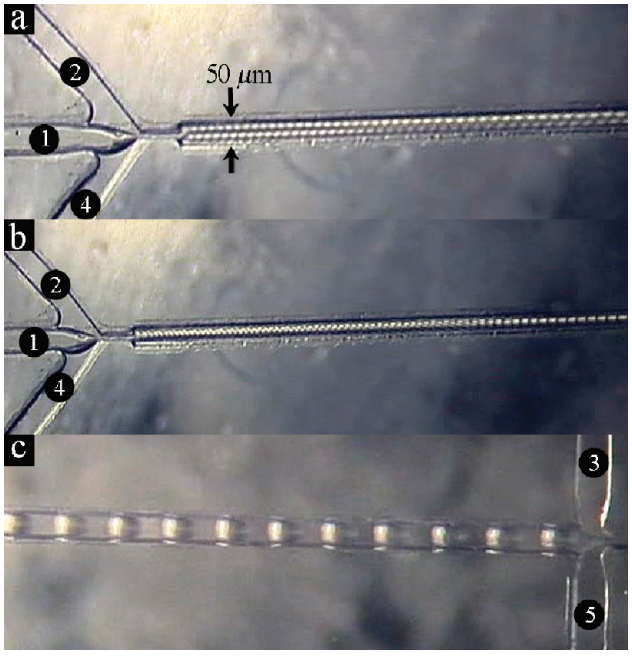

Figure 2. H_2O_2 aqueous droplets with different sizes in the TPGDA emulsion area. (a) TPGDA precursor with 15 μm H_2O_2 aqueous droplets; the flow rates for Q_1, Q_2, and Q_3 are 0.04, 0.33, and 0.15 mL/h, respectively. (b) TPGDA precursor with 30 μm droplets; the flow rates for Q_1, Q_2, and Q_3 are 0.04, 0.24, and 0.15 mL/h, respectively. (c) TPGDA precursor with 50 μm droplets; the flow rates for Q_1, Q_2, and Q_3 are 0.04, 0.17, and 0.15 mL/h, respectively. Here, the PVA concentration is 7 wt %.

loaded NOA 61 microspheres were dialyzed in a mixture of methanol and water to remove FITC residue. At last, all the particles were baked at 60 °C for 2 h.

Measurement and Characterization. The contact angle was measured by a contact angle goniometer (Rame-hart). The contact angle of NOA 61, EGDMA, and TPGDA precursor on the PDMS surface as measured is 63.8°, 36°, and 36.5°, respectively. For MCS and H_2O_2 solution, this value is 99.2° and 99°. Thermogravimetric (TG) and differential scanning calorimetry (DSC) analysis was performed on a TGA Q5000 analyzer and a TA Q1000 calorimeter at heating rate of 5 °C/min in a nitrogen atmosphere. The morphology of the microspheres was visualized on a JEOL-6700F SEM with a target acceleration voltage of 5 kV. Microscopic analysis was collected with a charge coupled device (CCD) camera (DP70, Olympus) mounted on an inverted microscopy (IX70, Olympus). Fluorescence observation was performed on a reflected fluorescence system equipped with an U-LH100HGAPO lamp housing and a IX2-RFACA motorized fluorescence mirror unit cassette (Olympus).

Results and Discussion

Droplet Formation and Emulsification. In the emulsion area, the polymer precursors from inlets 2 and 4 will first sheared the inner fluids from inlet 1 into droplets. The contact angle measurement indicates that precursors from inlets 2 and 4 have higher affinity for the PDMS surface than fluids from inlet 1. The precursors from channels 2 and 4 will wet the wall of the PDMS channel and shear MCS or H_2O_2 solution into droplets. Thus, aqueous droplets, in their flow, will be fully surrounded by NOA 61, EGDMA, or TPGDA precursor to form water-in-precursor emulsion.[54,55] After the formation of droplets in emulsion area,

(46) Massart, R. *IEEE Trans. Magn.* **1981**, *17*, 1247–1248.
(47) Gong, X.; Peng, S.; Wen, W.; Sheng, P.; Li, W. *Adv. Funct. Mater.* **2009**, *19*, 292–297.
(48) Bhattacharya, A.; Ray, P. *J. Appl. Polym. Sci.* **2004**, *93*, 122–130.
(49) Kim, N.; Sudol, D.; Dimonie, V. L.; El-Aasser, M. S. *Macromolecules* **2003**, *36*, 5573–5579.
(50) Yang, B.; Takahashi, K.; Takeishi, M. *Ind. Eng. Chem. Res.* **2000**, *39*, 2085–2090.
(51) Fruhner, H.; Wantke, K. D.; Lunkenheimer, K. *Colloids Surf., A* **1999**, *162*, 193–202.
(52) Xia, Y.; Whitesides, G. M. *Annu. Rev. Mater. Sci.* **1998**, *28*, 153–184.
(53) Niu, X.; Zhang, M.; Peng, S.; Wen, W.; Sheng, P. *Biomicrofluidics* **2007**, *1*, 044101.
(54) Chang, F. C.; Su, Y. C. *J. Micromech. Microeng.* **2008**, *18*, 065018.
(55) Seo, M.; Nie, Z.; Xu, S.; Mok, M.; Lewis, P. C.; Graham, R.; Kumacheva, E. *Langmuir* **2005**, *21*, 11614–11622.

Table 1. Relationship between Flow Rates of Different Fluids and H_2O_2 Droplet Size and Number[a,b,c]

fluid type	1 core	2 cores	3 cores	5 μm core	10 μm core	20 μm core
TPGDA precursor (Q_2 and Q_4)	0.15	0.15	0.15	0.5	0.4	0.3
H_2O_2 solution (Q_1)	0.06	0.07	0.09	0.04	0.04	0.04
silicon oil (Q_3 and Q_5)	0.1	0.11	0.12	0.15	0.15	0.15

[a] 1 core means one droplet of H_2O_2 solution encapsulated inside the TPGDA precursor. The rest have the analogous meaning. [b] 5 μm core means the droplet diameter of H_2O_2 solution encapsulated inside the TPGDA precursor is 5 μm. [c] The unit for flow rates is mL/h. The PVA concentration is 7 wt %.

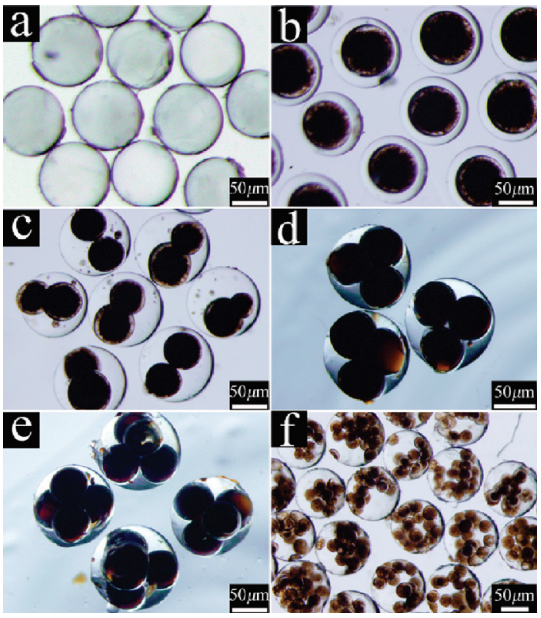

Figure 3. Optical microscope images of the NOA 61 encapsulating MCS microspheres with (a) none, (b) single, (c) dual, (d) triple, (e) quadruple, and (f) multiple magnetic aqueous droplets encapsulated insides.

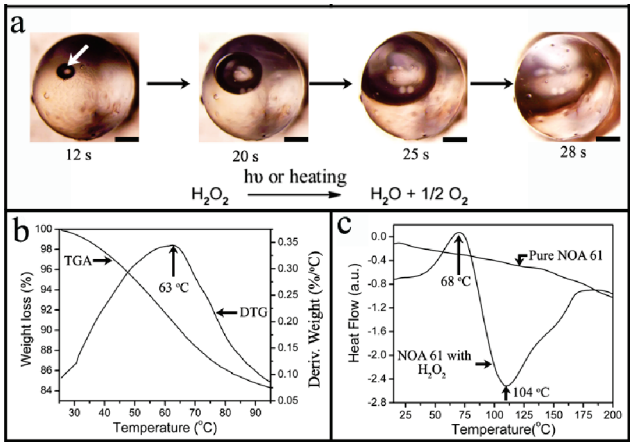

Figure 4. (a) Microscopic analysis to demonstrate the evolution of the interior structure of NOA 61 precursor encapsulating H_2O_2 droplet by UV exposure. Photos were extracted from a video. Scale bar is 25 μm. The lower panel shows the decomposition reaction of H_2O_2 under UV irradiation or heating. (b) TGA and DTG result for NOA 61 precursor encapsulating H_2O_2 droplets. (c) DSC result for pure NOA 61 precursor and NOA 61 precursor encapsulating H_2O_2 droplets.

the carrying fluid from inlets 3 and 5 further sheared the continuous fluid into droplets, as shown in Figure 1b. We used three syringe pumps to control the flow rates into inlets 1 (Q_1), 2 and 4 ($Q_2 = Q_4$), and 3 and 5 ($Q_3 = Q_5$). The droplet number inside the final microspheres could be adjusted by varying the flow rates of Q_3 and Q_5. For example, to prepare NOA 61 precursor

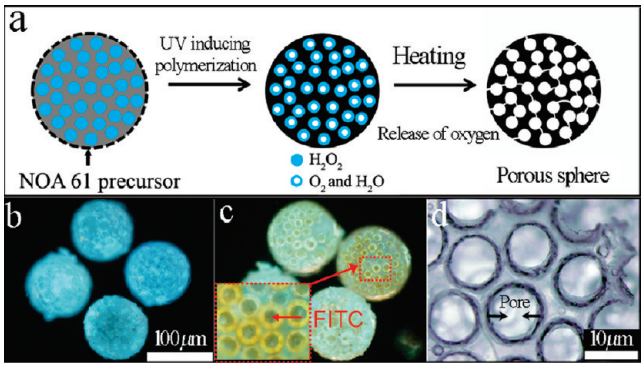

Figure 5. (a) Schematic picture to illustrate the structural evolution from emulsion to porous polymer. (b) FITC labeled H_2O_2 solution encapsulated by NOA 61 precursor. (c) After UV irradiation and heating, color change in the particles can be seen under fluorescence microscopy (the dashed frame shown in (c) shows the magnified image). This change is induced by the decomposition of H_2O_2 and subsequent removal of methanol and water. The original sites of FITC labeled H_2O_2 droplets were substituted by the solid FITC (red arrow). After heating, the polymer turns a little yellow as one can detect each yellow chamber encapsulating FITC. (d) After the dialysis process, the cross section of the microspheres is seen to have pores that are ~10 μm in diameter.

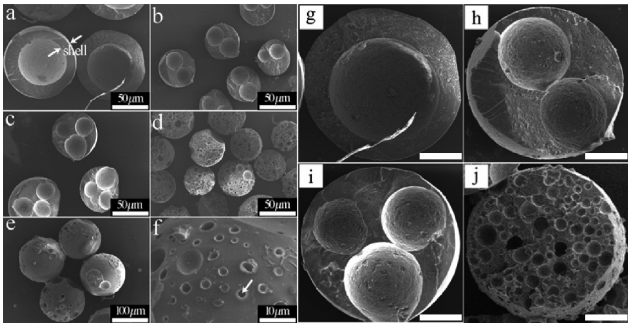

Figure 6. Sectional view of (a) single, (b) dual, (c) triple, and (d) multiple cores. (Samples were prepared by squeezing the particles with a glass slide.) The white arrows mark the shell. (e) Surface morphology of polyTPGDA porous particles and (f) the small pores distributed on the particle surface are several micrometers across (white arrow), formed by the release of oxygen. (g)−(j) are amplified pictures corresponding to (a)−(d). The scale bar in (g)−(j) is 50 μm.

with one (Figure 1c), two (Figure 1d), or multiple MCS cores (Figure 1e), we decreased the flow rate of Q_3 and Q_5 while fixed Q_1 and Q_2. The droplet size of MCS or H_2O_2 solution could also be adjusted by controlling the relative flow rates of Q_1, Q_2, and Q_4. For example, to prepare TPGDA precursor with 15 μm (Figure 2a), 30 μm (Figure 2b), or 50 μm H_2O_2 aqueous droplets (Figure 2c), we decreased the flow rate of Q_2 and Q_4 while fixed Q_1 and Q_3. The flow rates necessary to generate TPGDA precursor with a controlled number of encapsulated H_2O_2 aqueous droplets as well as their size are summarized in Table 1.

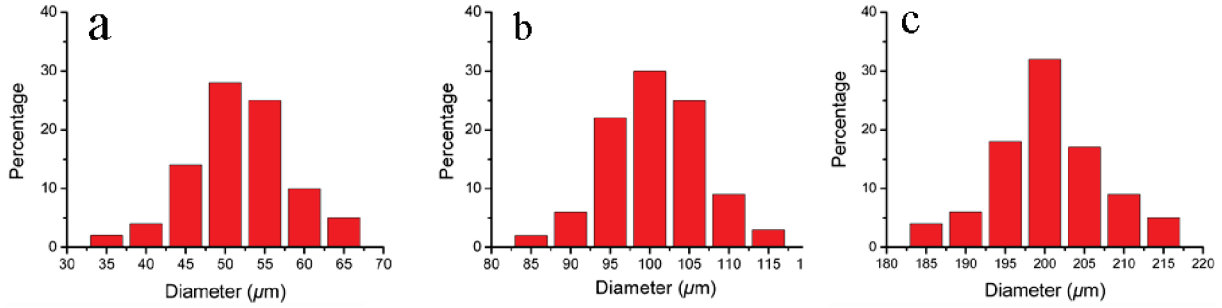

Figure 7. Size distributions of porous polyTPGDA microspheres with mean diameter of (a) 50, (b) 100, and (c) 200 μm. The distribution of sizes was determined by examining 200 microspheres using optical microscopy.

Solidification of Droplets. After droplets with desired number of cores were formed, they were exposed to UV irradiation (ELC-450 UV light spot-cure system, UV output 5 W/cm^2 at 365 nm) for ~30 s, under which condition polymerization (Scheme 1a−c) took place and fixed the structure of spheres, as seen in Figure 3. The outlet of chip was connected with a tygon tubing (i.d. 254 μm, Cole-Parmer Co.) which was immersed into a container filled with oleic acid for preparation of NOA 61 microspheres or silicon oil for polyEGDMA and polyTPGDA microspheres. To prepare particles bigger than 50 μm in diameter, we applied the UV irradiation directly on 254 μm Tygon tubing where the shape of droplets relaxed to spheres in the bigger sized tube. We selected oleic acid or silicon oil as receiver because carrying fluid paraffin or silicon oil can be dissolved into them. As a result, the microspheres flowing with carrying fluid can be easily transported to the receiver without stacking in the outlet.

Single-Pore Formation. Microspheres with controlled pore number inside were prepared by substituting MCS with H_2O_2 solution as aqueous core which will decompose under UV irradiation.[38−41] To determine how the pore was formed during the flow process, we took out one droplet of NOA 61 precursor encapsulating H_2O_2 solution while without applying UV irradiation in the channels. After UV irradiation under microscopy, we observed a hollowed zone diffusing (see the arrow in Figure 4a). The diffusion phenomenon started after 12 s exposure to UV and ended after 28 s and is probably caused by H_2O_2 decomposition (lower panel in Figure 4a). This means that after 30 s of UV exposure or long in the channels, we can directly obtain porous microspheres. Such phenomena can also be detected if we gradually heated the droplet with an increasing temperature. This is because both UV[12] and heat can lead to the decomposition of H_2O_2. Underlying it, we used DTG and DSC method to study the structural evolution of microspheres after 5 s UV irradiation. Figure 4b shows the TG and DTG result. From the DTG analysis, it was found that the microspheres lost their weight during the heat treatment and that there was a maximum in the rate of weight loss at around 63 °C. The DSC analysis of pure NOA 61 precursor and NOA 61 precursor encapsulating H_2O_2 microspheres is shown in Figure 4c. There are two peaks appearing: of which one is exothermic peak at 68 °C and another is endothermic peak at 104 °C. We attributed the first peak to exothermic decomposition of H_2O_2 and the second endothermic volatilization of water.[56,57] The DTG and DSC results proved that there was a chemical reaction taking place, and it must be the decomposition of the H_2O_2 because of the exothermic peak in DSC result and weight loss in DTG result.

Multiple-Pore Formation. To elucidate the formation of porous polymers, we loaded the H_2O_2 solution with yellow fluorescein isothiocyanate (FITC) methanol solution so as to make them detectable by fluorescence under microscopy. Figure 5a illustrates the structural evolution from multiple-core emulsion to porous polymers: (1) The microfluidic emulsification facilitates the formation of NOA 61 precursor with multiple encapsulated FITC-loaded H_2O_2 aqueous droplets (Figure 5b). (2) After UV irradiation the structure of the microspheres is solidified, simultaneous with the H_2O_2 decomposition. After heating at 60 °C, solvents such as water and methanol are removed, leaving behind only the FITC inside each small chamber (as arrow labeled in Figure 5c). The wall of the chamber is a little yellow (dashed frame in Figure 5c) since this kind of polymer usually turns to be a little yellow after heating. (3) After being dialyzed to remove the FITC, the porous interior can be observed. The dimension of the pores is about 10 μm, as seen in Figure 5d.

Polymer Microsphere Morphology. Figure 6 shows SEM pictures of polyTPGDA microspheres. Figures 6a−c shows the sectional views of crushed microspheres. We can see inside the structure the controlled number of hollowed pores after the decomposition of H_2O_2. Figure 6d is a sectional view of the porous polyTPGDA microspheres. The pore diameter can range from several micrometers to tens of micrometers. Figures 6e, f show the surface morphology of the particles, with small pores about several micrometers in diameter, formed by the release of oxygen. The maximum internal void volume was 70%, as calculated from the weight difference between the solid particles and porous particles of the same size. Figures 6g−j are the magnified pictures corresponding to Figures 6a−d. By this method, we also prepared poly EGDMA microspheres which had similar pore structure. The pores in NOA 61 microspheres (Figure 5c) seem more uniform than in poly TPGDA (Figure 6j). This may be caused by the higher viscosity of NOA 61 precursor that can efficiently prevent the aggregation of aqueous H_2O_2 droplets during droplets formation and solidification. By varying the flow rate of Q_3 and Q_5 while fixing Q_1, Q_2, and Q_4, microspheres with other sizes can be fabricated. Figures 7a−c show the size distribution of polyTPGDA microspheres with mean diameters of (a) 50, (b) 100, and (c) 200 μm. The size variance, defined as the standard deviation divided by the average particle diameter, is about 5%.

Conclusions

In the present experiment, we employed a microfluidic method to prepare porous microspheres. Photocurable polymer precursors were used to encapsulate the MCS in order to study the controlled formation of polymer microspheres with multiple encapsulated droplets. On the basis of that knowledge, we

(56) Wu, L. K.; Chen, K. L.; Cheng, S. Y.; Lee, B. S.; Shu, C. M. *J. Therm. Anal. Calorim.* **2008**, *93*, 115–120.
(57) Khoumeri, B.; Balbi, N.; Leoni, E.; Chiaramonti, N.; Balbi, J. H. *J. Therm. Anal. Calorim.* **2000**, *59*, 901–911.

replaced MCS by H_2O_2 solution. The interface between organic and aqueous phases in the emulsion was stabilized with a PVA surfactant. Owing to this interface, we could obtain a single particle containing multiple numbers of H_2O_2 droplets. Via the simultaneous UV-induced polymerization of the shell and the decomposition of H_2O_2, the precursors were solidified while oxygen was released, forming the porous structure. With the MMF method's controllable flow rate, not only the particle size but also the number and size of the pores inside the polymer are controllable. As H_2O_2 decomposition can be triggered by either UV irradiation or heat treatment, this method may also be useful in preparing porous materials that are thermally curable; however, further investigation is required.

Acknowledgment. This publication is based on work partially supported by Award No. SA-C0040/UK-C0016, made by King Abdullah University of Science and Technology (KAUST), Hong Kong RGC grants HKUST 603608 and 602007. The work was also partially supported by the Nanoscience and Nanotechnology Program at HKUST.